Chapter 3

Bituminous Coal Combustion with New Insights

Guan-Fu Pan, Hong-De Xia and Zhen-Yu Tian

Additional information is available at the end of the chapter

http://dx.doi.org/10.5772/64136

Abstract

As one of the most important primary energy, bituminous coal has been widely applied in many fields. The combustion studies of bituminous coal have attracted a lot of attention due to the releases of hazardous emissions. This work focuses on the investigation of combustion characteristics of Shenmu bituminous pulverized coal as a representative bituminous coal in China with a combined TG-MS-FTIR system by considering the effect of particle size, heating rate, and the total flow rate. The combustion products were accurately quantified by normalization and numerical analysis of MS results. The results indicate that the decrease of the particle size, heating rate, and the total flow rate result in lower ignition and burnout temperatures. The activation energy tends to be lower with smaller particle size, faster heating rate, and lower total flow rate. The MS and FTIR results demonstrate that lower concentrations of different products, such as NO, NO_2, HCN, CH_4, and SO_2, were produced with smaller particle size, slower heating rate, and lower total flow rate. This work will guide to understand the combustion kinetics of pulverized coals and be beneficial to control the formation of pollutants.

Keywords: bituminous coal, combustion characteristics, TG-MS-FTIR technique, particle size, heating rate, flow rate

1. Introduction

Coal is one of the most important primary energy for last whole century and future decades. As the foundation of the application of coal, the research on bituminous coal combustion has never been stopped. Different kinds of bituminous coals with multitudinous research instruments and methods for the investigation of coal combustion characteristics have been carried out for

years. Peng and Wu [1] studied the bromine release from bituminous coal during combustion. They used the sequential chemical extraction method to investigate the modes of occurrence of bromine in bituminous coal by a tube furnace. The results showed that the bromine release rate increased with the increase of temperature, and 500–900°C was the main stage of bromine release. They also concluded that water vapor can promote the Br release and the additive of SiO_2 can capture the bromine effectively in the process of the coal combustion. Tsuji et al. [2] studied the combustion emission of one bituminous coal from Australia and two high-ash coals from South Africa on different blending ratios by an advanced low NO_x burner. They concluded that the NO_x emission characteristic from bituminous coals was similar to these two high-ash coals. The combustion efficiencies on the bituminous coals were higher than those of the high-ash coals. Molina and Shaddix [3] studied the influence of enhanced oxygen levels and CO_2 bath gas on single-particle pulverized coal ignition of a U.S. eastern bituminous coal. For the ignition process observed in the experiments, the CO_2 results were explained by its higher molar specific heat and the O_2 results were explained by the effect of O_2 concentration on the local mixture reactivity. The experiments showed that a lower O_2 concentration and the presence of CO_2 increased the ignition delay time but had no measurable influence on the time of complete volatile combustion. Gao et al. [4] performed an online analysis of the soot emissions from the Inner Mongolia bituminous coal combustion and pyrolysis processes with a vacuum ultraviolet photoionization aerosol time-of-flight mass spectrometer. They concluded that at lower oven temperatures (<873 K), the soot particles generated in combustion processes contained more oxygen-containing PAHs (O-PAHs). At high temperatures, however, the soot particles from combustion contained mainly PAHs without any functional groups. Yu et al. [5] studied the characteristics of char particles and their effects on the emission of particulate matter (PM) from the combustion of a Chinese bituminous coal in a laboratory-scale drop tube furnace. The coal samples were subjected to combusted in 20 and 50% O_2 at 1373, 1523, and 1673 K, respectively. The results showed that coal particle size and pyrolysis temperature had a significant influence on the char characteristics. The influence of combustion temperature on supermicron-sized PM emission greatly depended on the oxygen concentration. Among various kinds of bituminous coals, the Shenmu bituminous coal (SBC) has been adopted as one of the most widely used bituminous coals in China [6–8] since it has the advantages of excellent thermal stability, high calorie, and huge reserves. The investigation of the combustion characteristics is essential to understand the combustion process and control the pollutant products.

In recent years, SBC has been studied in terms of its burning and gasification properties. In 2003, Sun et al. investigated the thermogravimetric (TG) characteristics of SBC and reported that vitrinite had higher volatile matter yield, maximum weight loss rate, and lower initial decomposition temperature and peak temperature than that of inertinite. Compared to pressure and heating rate, the temperature has a more important impact on the devolatilization of SBC [9]. With TG analysis, Zhao et al. studied the ignition temperature (T_{ig}), maximum reaction temperature (T_{max}), burning rate, burnout temperature (T_{burn}), and combustion features of SBC coal and coke fine mixed sample. The results showed that with the increase in the coke fine content, T_{ig} of the coal and coke fine mixture, the caloric value of the sample, and T_{max} would increase, while the burning rate would decrease [10]. Yang et al. studied the SBC ash's physicochemistry with temperature on the basis of TG-differential scanning colorimetry

(TG-DSC) methods. The results indicated that the SBC ash could convert into an eutectic at low temperatures [11]. Chang et al. investigated the formation of nitrogenous products from the gasification of SBC in a fluidized-bed/fixed-bed reactor [7]. More recently, Yang et al. investigated the SBC's characteristics of combustion and nitrogen oxide (NO_x) release in a fixed-bed reactor [12]. The composition of the flue gas was analyzed to investigate the effect of sodium acetate on the combustion process and NO_x emission. Sodium acetate was observed to reduce NO_x emissions due to their special reactions with the nitrogen-containing species [12]. Even though the maceral groups, characteristic temperature, ash's physicochemistry, and nitrogenous products of SBC have been studied, a systematic study regarding the most important conditions such as the effect of particle size, heating rate, and total flow rate on its combustion characteristics is scarcely available in the literature. Mass spectrometry (MS) and Fourier transform infrared spectroscopy (FTIR) are widely used in multicomponent analysis in energy chemical industry and are suitable to be combined with TG and the gas chromatographic method [13]. It is efficient and reliable to use the TG-MS-FTIR system for numerical analysis of the combustion characteristics of coal. In the current work, the combustion characteristic of SBC was comprehensively studied with the online TG-FTIR-MS system. The products formed in the combustion of SBC were accurately qualified and quantified by considering the electron impact ionization cross sections, ion flow intensities, and the partial pressures of different species. The condition-characteristic relationship among the particle size, heating rate and total flow rate and ignition, and burnout temperature as well as activation energy was addressed. With the comprehensive use of TG-FTIR-MS, the detailed combustion characteristics of SBC have been presented for the first time. Such strategy will supply a significant guidance for the real use of SBC and other solid fuels in the future.

2. Materials and methods

2.1. Coal samples

The SBC samples were bought from Shenmu Energy Developments Ltd Company and grinded into powder with different sizes. Before test, the sample was put into drying oven at a temperature of 105°C for 90 min. Then, the coals were sieved to a particle size of lesser than 40, 90–100, 128–180, 280–355, and 355–500 μm. To identify the phases of SBC, X-ray diffraction (XRD) patterns were recorded using Bruker D8 Focus at 40 kV and 150 mA with Cu Kα (λ = 0.154056 nm) radiation. By referring to the Joint Committee on Powder Diffraction Standards (JCPDS) database cards which have also been called power diffraction file (PDF), the crystalline phases were identified. The samples were scanned in step of 0.02° (2θ) over the range of 5–90°. By comparing with standard PDF, it was found that the coal samples are mainly composed of $CaCO_3$, SiO_2, and kaolinite as shown in **Figure 1**. The existence of carbonate could be the main reason to form the weak weight loss peak at the end of the combustion processes.

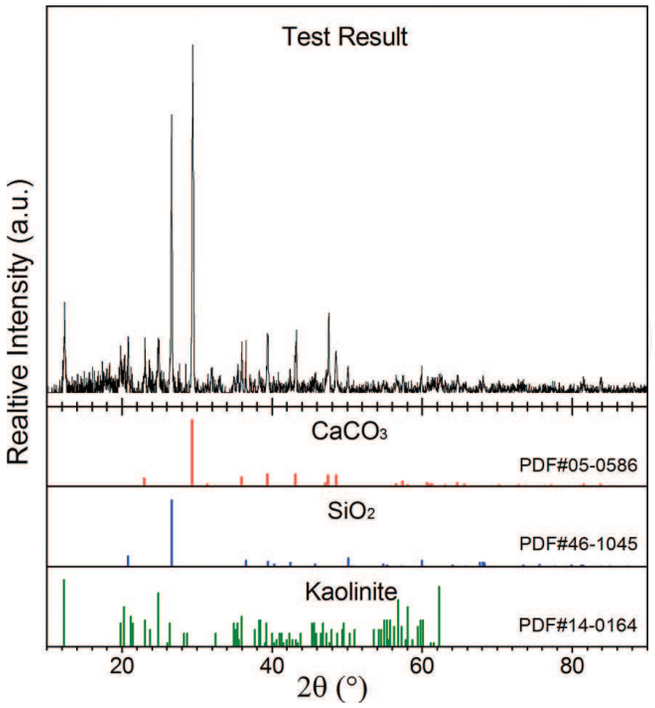

Figure 1. XRD patterns of SBC.

The elements of SBC samples were identified by the coal proximate analyzer as shown in **Table 1**. M_{ad}, A_{ad}, V_{ad}, FC_{ad}, and $Q_{ad.net}$ represent the moisture, ash, volatile, fixed carbon, and low calorific capacity in air-dried basis, respectively. C_{ad}, H_{ad}, O_{ad}, N_{ad}, and S_{ad} represent carbon, hydrogen, oxygen, nitrogen, and sulfur elements in air-dried basis, respectively.

Proximate analysis					Ultimate analysis				
M_{ad} (%)	A_{ad} (%)	V_{ad} (%)	FC_{ad} (%)	$Q_{ad.net}$ (kJ/kg)	C_{ad} (%)	H_{ad} (%)	O_{ad} (%)	N_{ad} (%)	S_{ad} (%)
6.53	10.41	32.40	50.66	26,120	66.70	4.11	10.79	1.04	0.42

Table 1. The proximate analysis and ultimate analysis results of SBC.

2.2. Comprehensive test

The tests of SBC combustion characteristics were performed with the TG-MS-FTIR system which comprises a TG analyzer (STA-449F3, Netzsch), a mass spectrometer (QMS403C, Aeolos), and an FTIR spectrometer (Tensor 27, Bruker). The combined system was controlled simultaneously and data were recorded by a computer as shown in **Figure 2**. Due to the TG's limit of highest heating temperature and heating rate, the highest heating temperature was set at 1200°C and the heating rate were set at 10, 20, 30, and 40°C/min. Considering the oxygen demand for complete combustion of 10 mg SBC samples within the limitations of TG, the total flow rates were set at 50, 100, and 150 sccm. The tests were carried out in four steps. First, an SBC sample of about 10 mg was dispersed on a circular alumina pan and the air in TG chamber

http://dx.doi.org/10.5772/64136

was replaced with a gas mixture which consists of 20% O_2 and 80% Ar. The supplied O_2 was much more than the theoretically needed for the complete oxidation of the SBC sample but was similar to the air. Second, the samples were heated with a heating rate of 10°C/min from 40 to 110°C and kept for 30 min. Third, the samples were heated to 1200°C by four heating rates, namely, 10, 20, 30 and 40°C/min, respectively. Finally, the whole temperature-rising program was finished after an isothermal process of 10 min. Three total flow rates (50, 100, and 150 sccm) containing 20% O_2 and 80% Ar were sent into the TG chamber during the whole heating processes. The detailed experimental conditions are summarized in **Table 2**.

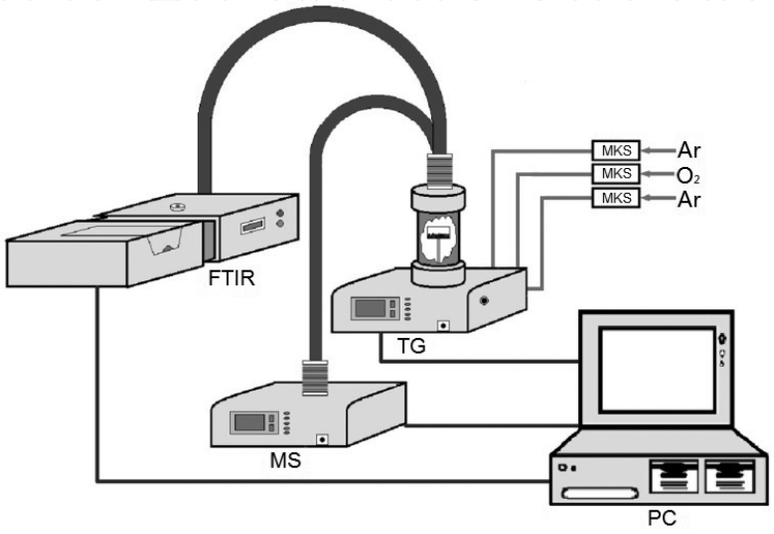

Figure 2. Scheme of the TG-MS-FTIR system.

Condition	Mass (mg)	Flow rate (sccm)			Heating rate (°C/min)	Particle size (μm)
		O_2	Ar	Ar		
1	9.411	20	60	20	20	0–40
2	10.248	20	60	20	10	90–100
3	9.788	20	60	20	20	90–100
4	9.348	20	60	20	30	90–100
5	9.589	20	60	20	40	90–100
6	9.251	20	60	20	20	125–180
7	10.246	20	60	20	20	280–355
8	9.786	20	60	20	20	355–500
9	9.341	10	20	20	20	90–100
10	9.864	30	100	20	20	90–100

Note: Protective gas of TG is 20 sccm Ar constantly.

Table 2. Experimental conditions.

2.3. Data treatment

2.3.1. Characteristic temperature

The ignition characteristic of SBC is analyzed based on T_{ig}. In the present work, T_{ig} is determined by the commonly recognized TG-DTG methods [14]. T_{burn} is defined as the temperature with 98% total weight loss. T_{max}, referring to the temperature at which combustion product own maximum volumetric flow, was also determined through numerical analysis.

2.3.2. Kinetic analysis

The combustion kinetic parameters from TG data are calculated by the Coats-Redfern method [15]:

$$n = 1,\ldots \ln[\frac{-\ln(1-\alpha)}{T^2}] = \ln\frac{AR}{\beta E}(1-\frac{2RT}{E}) - \frac{E}{RT} \tag{1}$$

$$n \neq 1,\ldots \ln[\frac{1-\ln(1-\alpha)^{1-n}}{T^2(1-n)}] = \ln[\frac{AR}{\beta E}(1-\frac{2RT}{E})] - \frac{E}{RT} \tag{2}$$

where $\alpha = (m_0 - m)/(m_0 - m_\infty)$ is the weight loss ratio; m refers to the sample mass; m_0 and m_∞ represent the initial mass and the final mass, respectively; β is heating rate, K·min^{-1}; $R$is the gas constant; E stands for activation energy, J·mol^{-1}; A is the frequency factor, min^{-1}; and n refers to the order of reaction. In general, the item $\frac{2RT}{E} << 1$ and $(1 - \frac{2RT}{E}) \approx 1$. As the first item of the right side of equations is nearly a constant, the two equations should result in a straight line of slope. E can be deduced through calculation with the slope.

2.3.3. Products analysis

To obtain the volumetric flow rates of the products during the oxidation of SBC, both MS and FIIR were used. In order to provide accurate quantitative analysis, a novel method of equivalent characteristic spectrum analysis was employed and the details of such method can be found elsewhere [16]. In the MS analysis, argon was used as a reference gas to calibrate the products by considering the electron impact ionization cross sections, ion flow intensities, and the partial pressures of different species. The characteristic spectra and relative sensitivity were deduced. The effect of initial coal weight on the formation of products was excluded by normalization of the coal weight.

Derivative thermogravimetry (DTG) curve is a very important result of SBC because DTG can reflect the change of combustion rate directly and it was related to the acquirement of ignition temperature, burnout temperature, and combustibility index. Since the mass loss of sample mainly comes from the decomposition of volatiles in the coal samples, the DTG calculated from

http://dx.doi.org/10.5772/64136

MS results of combustion products should be consistent with the DTG results measured by TG analyzer. As a representative, **Figure 3** compares the DTG curve calculated from MS results and measured TG results under condition 4 (see **Table 2**). The results indicate that the calculated MS results are in good agreement with the measured ones. The relative uncertainty was estimated to be ±2.6% [16].

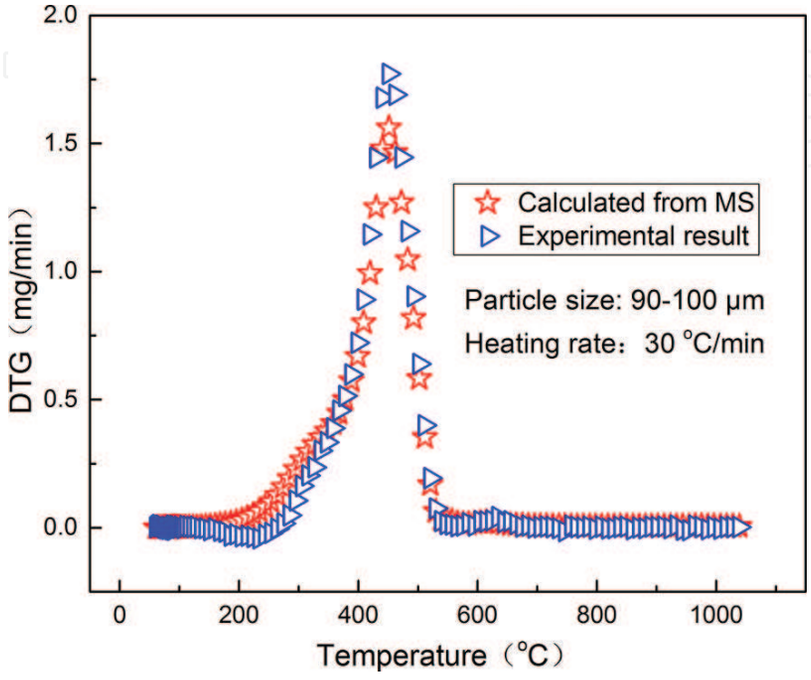

Figure 3. Comparison of DTG curves from calculation and experiment.

3. Results and discussion

3.1. TG/DTG results

Figure 4 presents the TG/DTG curves obtained in the combustion of SBC samples. As temperature increases, the coal sample could proceed with several steps, including devolatilization, coke formation, and coke combustion. The peak of maximum weight loss moves toward high temperatures gradually and the peak value decreases slightly as the particle size increases. The combustion rate depends on the diffusion and reaction ability. During the rapid combustion processes, the major factor affecting the combustion is diffusion ability. As the particle size increases, the contact surface area decreases, which would inhibit the diffusion of oxygen and make the devolatilization and combustion difficult. As a consequence, the devolatilization occurs at higher temperatures and the value of weight loss peak decreases.

Compared to particle size, heating rate has more apparent effect on the characteristics of weight loss. As the heating rate increases, the peak of weight loss moves toward high temperatures. In addition, the peak values and residues decrease as well. Since diffusion ability is the

dominant factor in affecting the combustion process, longer contact time of sample surface and oxygen could contribute to SBC conversion. Furthermore, longer time is needed to reach the same temperature at slower heating rate relative to faster one. For instance, the time needed to reach 1200°C at 10°C/min is four times as the time needed to reach 1200°C at 40 °C/min. Thus, the burnout time with low heating rate is longer. Sufficient contact of particles and oxygen is beneficial for the combustion process, and the maximum value of weight loss occurred at lower temperatures and the maximum weight loss shifted to larger values [17]. It is clear that there is a small weight loss peak within 600–700°C. This weak peak could come from the decomposition of carbonate in the coal samples. In addition, the TG/DTG results of different total flow rates are observed to be quite similar as displayed in **Figure 4c**. As the oxygen supplied is much more than that theoretically needed for the complete combustion, the weight loss characteristics are insensitive to the diverse total flow rate changed in experiments.

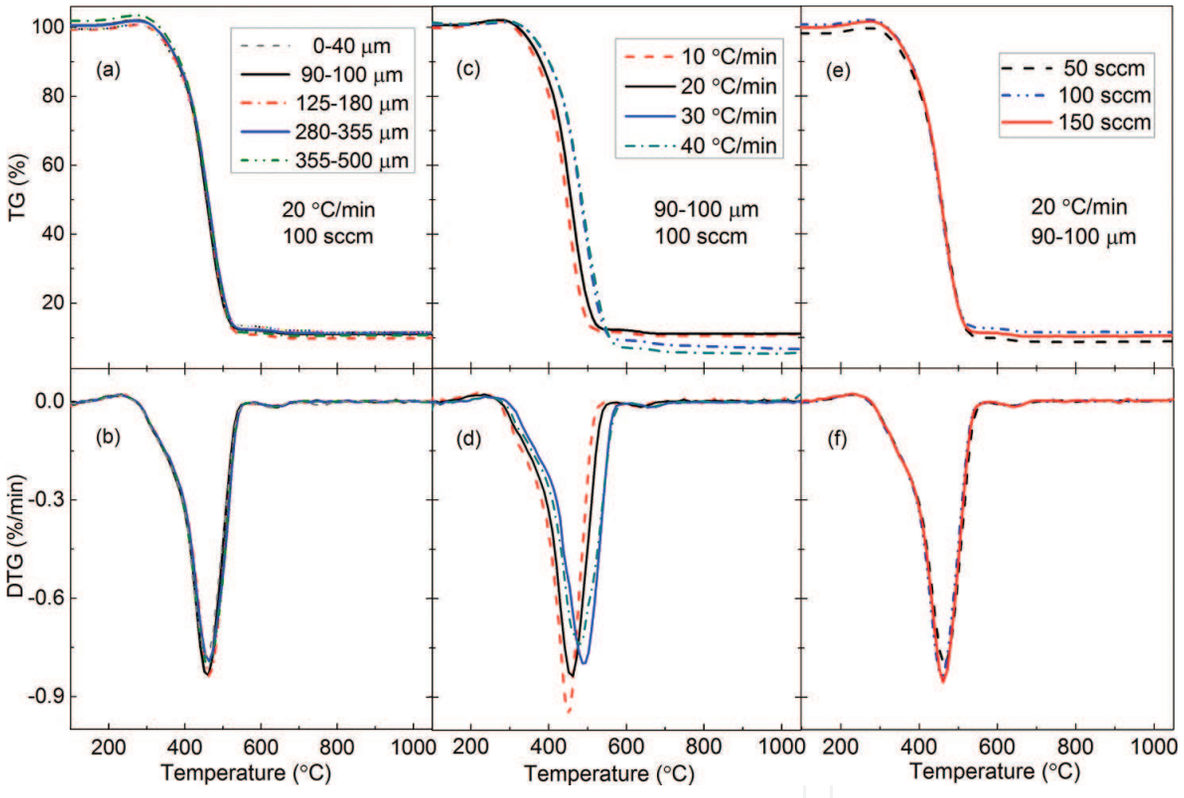

Figure 4. TG and DTG curve of SBC combustion with different particle sizes, heating rates, and total flow rates.

3.2. Characteristic temperatures

The characteristic temperatures obtained in the combustion of SBC at different particle sizes, heating rates, and total flow rates are shown in **Figure 5**. As indicated in **Figure 5a**, both T_{ig} and T_{burn} fall down as the particle size decreases, which is consistent with the results reported by Zhang et al. [18] for Yuanbaoshan and Datong coal and Zhou et al. [19] for Lengshuijiang

coal and lean coal. According to Zhang et al. and Zhou et al., the decrease of particle size could lead to larger surface area to expose to oxygen. The same behavior could occur to SBC and the larger surface area of SBC sample with smaller particle size would endow it with lower T_{ig} and T_{burn}.

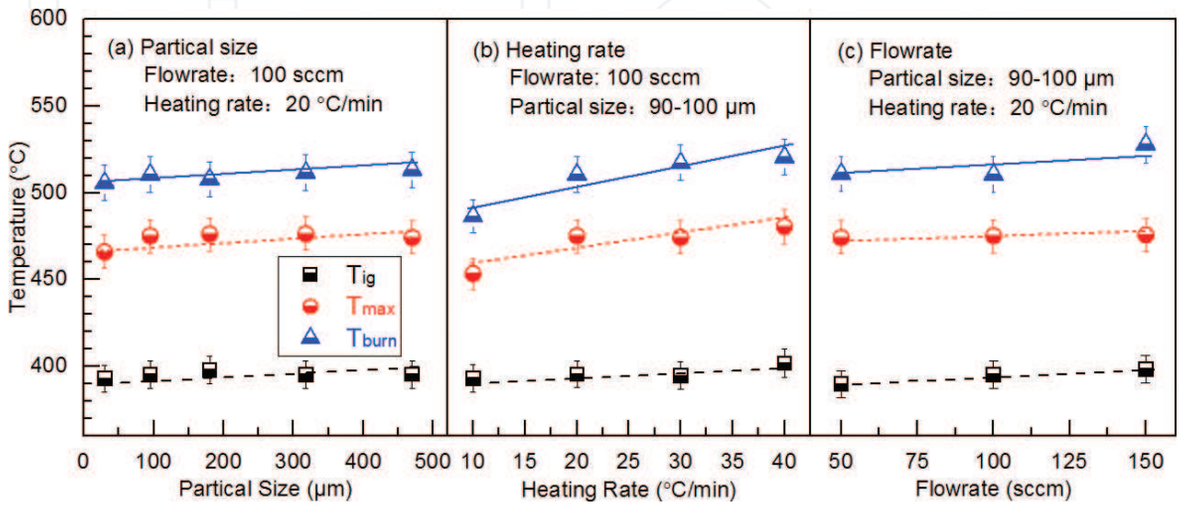

Figure 5. Characteristic temperatures of SBC combustion with different particle sizes, heating rates, and total flow rates.

Figure 5b displays the characteristic temperature as a function of heating rate. T_{ig}, T_{max}, and T_{burn} tend to decrease slightly as the heating rate decreases, which agrees well with the conclusion drawn by Lu et al. [20] for Qilianta coal. This is due to the fact that the thermal conduction in coal particle at lower heating rate is better than that at higher ones. With the increase in temperature, the diffusion becomes better, which is helpful to the devolatilization and results in lower T_{ig}. Moreover, the reaction time is more sufficient at slower heating rate. As the plugging of the surface pores is avoided, it is more difficult to form ash cladding, which could give rise to a lower T_{burn} [21].

For the total flow rate, a slight increase of T_{ig} is observed with large total flow rate (see **Figure 5c**). This slight increase mainly comes from shorter residence time of O_2 on the surface of coal particles at higher total flow rates. Even though more oxygen reached the coal surface, the higher speed of oxygen molecule makes the adsorption of oxygen more difficult. As the supplied O_2 was much more than the theoretically needed for the complete oxidation of the SBC sample, the influence of oxygen flow on the complete combustion and maximum combustion speed is not obvious. As a consequence, both T_{max} and T_{burn} exhibit similar values in the combustion of SBC at different total flow rates.

3.3. Activation energy

Figure 6 summarizes activation energy (E) of SBC with variation of particle size, heating rate, and total flow rate. E tends to be low with the increase in the heating rate, decrease in the

particle size, and the total flow rate. As the particle size decreases, the surface area increases, which would result in more contact area with oxygen and better thermal reactivity. Thus, energy transfer from outside to inside rapidly increases, and the value of E decreases. When the total flow rate increases, the contact time of oxygen and sample surface will be shortened and the value of E increases. On the other hand, the temperature will rise quickly with fast heating rate and the oxidation of coal could become easier. The lower energy barrier makes the oxidation easier [22–24]. This finding also shows good agreement with the conclusion drawn by Lu et al. [20] for different kinds of coals. Similar to the tendency of T_{ig}, E decreased when the total flow rate turned lower. The adsorbability of oxygen on the coal particle surface is better with lower total flow rate, which could be responsible for the decrease in the energy barrier.

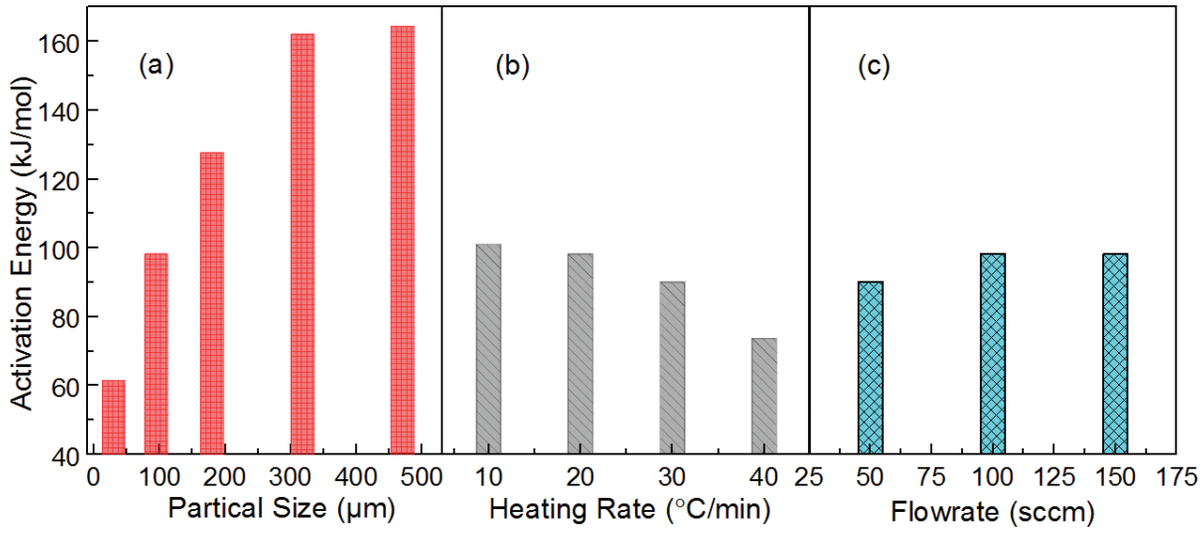

Figure 6. Activation energies of SBC combustion with different particle sizes, heating rates, and total flow rates.

3.4. MS and FTIR results

The volumetric flows of different combustion products at different temperatures can be obtained by normalization and numerical analysis of MS results. The maximum volumetric flows of different combustion products as well as the corresponded temperatures (T_m) are used to explore the formation rule of emitted pollutants. **Table 3** shows the maximum volumetric flows of CH_4, NH_3, NO, HCN, NO_2, and SO_2 as well as the corresponded T_m. By comparing the results obtained with different particle sizes, the listed species tend to be less produced with smaller particle sizes. In view of the heating rate, lower amounts of these products were measured at lower heating rate. As far as the total flow rate is concerned, the quantity of these species becomes lower when the total flow rate is smaller. In general, T_m is insensitive to the particle size. However, the increase in the total flow rate normally results in smaller T_m. With the increase in the heating rate, T_m of NO, NH_3, and HCN tends to be higher, while T_m of SO_x becomes lower. To summarize, lower concentrations of CH_4, NH_3, NO, HCN, NO_x, and SO_2 were observed at smaller particle size, slower heating rate, and higher total flow rate.

http://dx.doi.org/10.5772/64136

No.	CH_4		NH_3		NO		HCN		NO_2		SO_2	
	Value (slm)	T_m (°C)	Value (slm)	T_m (°C)	Value (slm)	T_m (°C)	Value (slm)	T_m (°C)	Value (slm)	T_m (°C)	Value (slm)	T_m (°C)
1	4.08E−05	442	3.61E−04	318	4.72E−05	493	5.05E−04	452	6.14E−05	431	6.38E−06	400
2	3.53E−05	427	2.41E−04	309	3.56E−05	458	3.68E−04	443	4.17E−05	438	4.52E−06	402
3	5.91E−05	440	2.81E−04	305	7.69E−05	492	3.09E−04	451	6.41E−05	440	7.73E−06	388
4	6.51E−05	437	2.17E−04	307	6.46E−05	494	4.94E−04	453	9.84E−05	429	8.37E−06	379
5	5.06E−05	430	3.41E−04	337	1.40E−04	507	3.97E−04	512	1.29E−04	439	1.24E−05	350
6	7.27E−05	453	4.23E−04	338	4.60E−05	494	6.74E−04	463	7.10E−05	442	4.55E−06	400
7	7.94E−05	453	4.89E−04	306	6.97E−05	504	5.19E−04	453	7.43E−05	442	6.33E−06	410
8	7.96E−05	432	3.73E−04	317	4.95E−05	503	4.52E−04	463	7.20E−05	442	6.20E−06	390
9	9.75E−05	453	7.72E−04	327	9.44E−05	504	6.53E−04	463	1.47E−04	453	1.01E−05	400
10	3.76E−05	430	1.58E−04	316	4.32E−05	482	3.03E−04	472	4.99E−05	440	5.75E−06	398

Note: T_m refers to the temperature at which the peak flow is obtained.

Table 3. Maximum volumetric flow of representative combustion products.

Figure 7 shows the volumetric flow rates of different species formed under condition 4 (see **Table 2**). In the combustion of SBC, both NH_3 and HCN exhibited two-peak shapes. The peak before T_{ig} comes from the devolatilization, whereas the peak after T_{ig} mainly results from the decomposition of nitrogen components in both coal volatile and char. Further increase in the temperature led to the conversion of the two species into NO and NO_2.

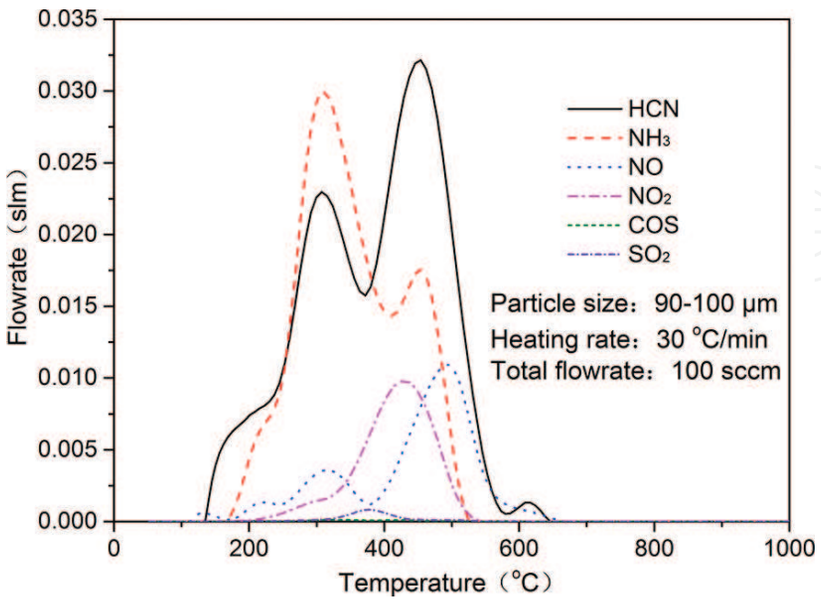

Figure 7. Flow rates of major products.

NO_2 exhibited a shoulder peak and an asymmetric single peak. The shoulder peak is due to the weak release of NO_2 during devolatilization. The asymmetric single peak could result from the conversion of nitrogen-containing heterocyclic species at the end of devolatilization and the beginning of char combustion. However, the other nitrogenous components enriched in char will release NO_2 during the rapid combustion of char. Less NO_2 emissions were observed at smaller particle size, slower heating rate, and higher total flow rate. Similarly, the emissions of SO_2 are relatively less than those formed with slower heating rate and higher total flow rate. However, the amount of SO_2 is quite similar for the investigated particle size range, indicating that it is insensitive to the particle size.

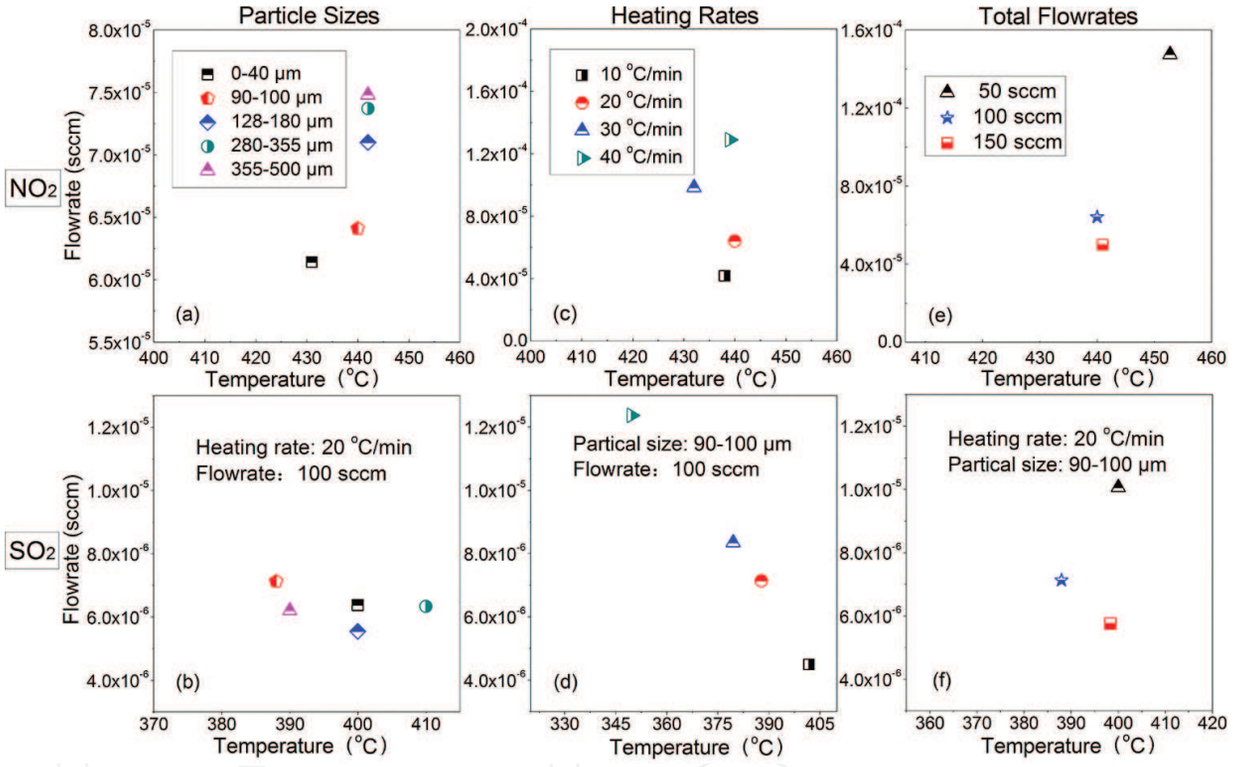

Figure 8. Production of NO_2 (a, c, e) and SO_2 (b, d, f) with different particle sizes, heating rates, and total flow rates.

By comparing the formation of NO_2 and SO_2 with different particle sizes, heating rates, and total flow rates shown in **Figure 8**, it is obvious that the amount of SO_2 production is much lower than those of NO and NO_2. To summarize, the SBC combustion with smaller particle size, slower heating rate, and higher total flow rate is beneficial to controlling the formation of pollutants. This finding is consistent with the results reported for Hegang, Tiefa, and Zhungeer coals by Wei et al. [25] and Heshan sulfur coal by Jiang et al. [23, 26].

To visualize the formation of the major species and avoid the effect of ion fragmentation in MS, FTIR with the spectral range of 500–5000 cm^{-1} was involved in the current work. **Figure 9** presents a representative three-dimensional (3D) spectrum measured with a particle size of 90–100 μm, a total flow rate of 100 sccm, and a heating rate of 20°C/min. The

http://dx.doi.org/10.5772/64136

maximum absorbance peak is located at the wave number of 2380 cm^{-1} corresponding to the anomalistic vibration of CO_2. Another obvious peak at 700 cm^{-1} belongs to the bending vibration of CO_2. The peaks at 1375 and 3600 cm^{-1} correspond to SO_2 and H_2O, respectively. By comparing the standard spectral peaks of different species, overlapped peaks were observed. For instance, the peak between 1500 and 1800 cm^{-1} should be the overlap of H_2O and NO [27, 28]. As can be seen in **Figure 9**, CO_2 becomes detectable at around 140°C. Up to 200°C, a slow increase was observed. Another turning point was measured at about 375°C, which also agrees well with the wave valley in the profiles of HCN and NH_3. Besides CO_2, the fast production of the major species was achieved within the temperature range of 400–500°C, which is consistent with the rapid combustion temperature revealed in the MS analysis. In order to show gradual change of specific species at different temperatures in **Figure 9**, **Figure 10** presents two-dimensional (2D) spectra. The peaks located at about 2380 and 3600 cm^{-1} correspond to the CO_2 and H_2O, respectively. By comparing different spectra obtained at different temperatures, it is obvious that the maximum peak values of different combustion products are located at the temperature of 450°C, corresponding to the rapid combustion temperature. The spectra obtained at temperatures higher than 450°C exhibit very weak peaks since the SBC samples were nearly burned out.

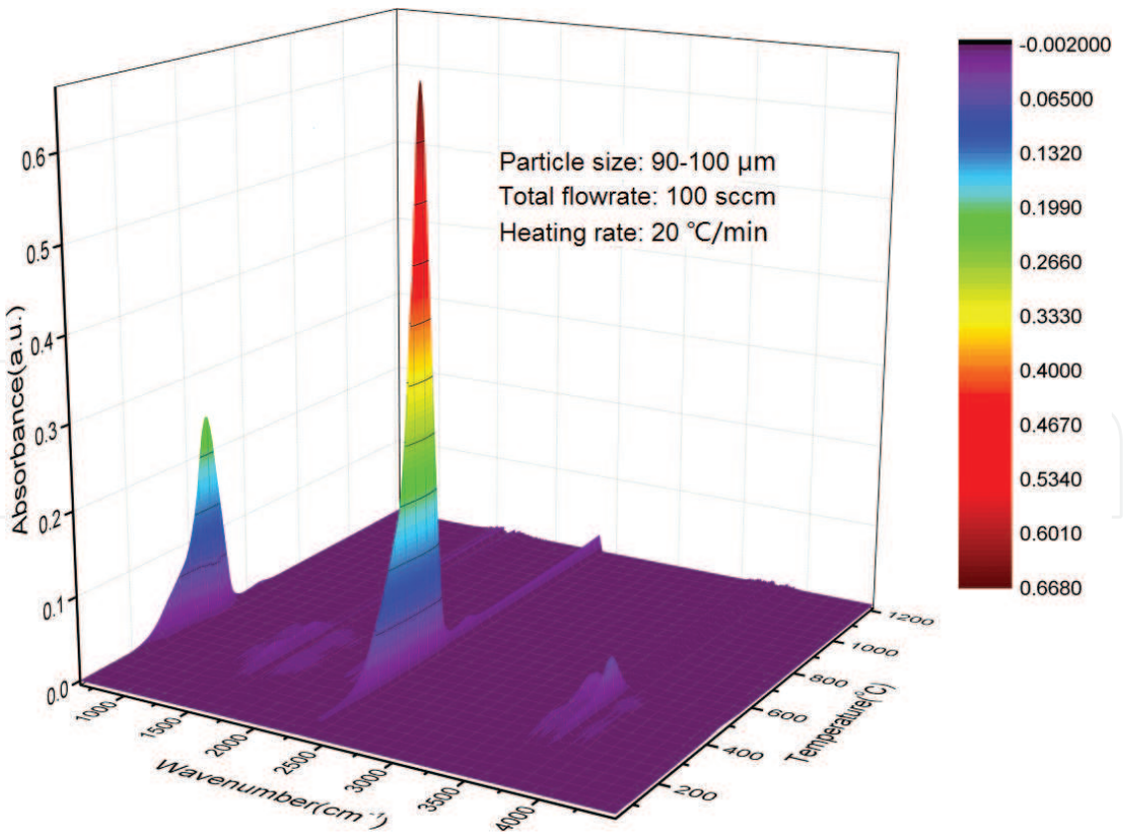

Figure 9. 3D FTIR spectra with different wave numbers and temperatures.

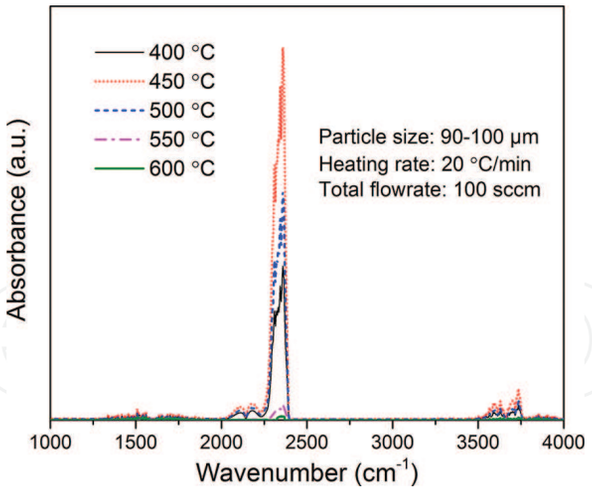

Figure 10. 2D FTIR spectra at different temperatures.

4. Conclusions

The combustion of SBC was comprehensively studied with the online TG-MS-FTIR system in terms of characteristic temperatures as well as qualitative and quantitative analyses of products. Five particle sizes ranging from 0 to 500 μm, four heating rates from 10 to 40°C/min, and three total flow rates from 50 to 150 sccm were used. To avoid the influence of overlap peaks, signal drift, and dynamic response delay in ion current spectra during MS analysis, argon was used as a reference gas to calibrate the products by considering the electron impact ionization cross sections, ion flow intensities, and the partial pressures of different species. The results indicate that the decrease in the particle size, heating rate, and flow rate lead to lower ignition and burnout temperatures, while the activation energy tends to be lower with smaller particle size, faster heating rate, and lower flow rate. The decrease in the particle size could lead to more contact area with oxygen and better thermal reactivity. Slower heating rate could provide more sufficient time for the reaction. Moreover, a higher total flow rate would reduce the oxygen adsorbability on the coal particle surface at a higher flow speed. From MS and FTIR analysis, lower concentrations of different products were observed to be formed at smaller particle size, slower heating rate, and higher total flow rate. These findings will guide to understand the combustion kinetics of SBC and be beneficial to control the formation of pollutants.

Acknowledgements

The authors thank the financial support from the Recruitment Program of Global Youth Experts and Strategic Priority Research Program of the Chinese Academy of Sciences (Grant No. XDA0703100). The authors also thank Mr. Kai Wei, Mr. Zhi-Qiang Gong, and Dr. Zhi-Cheng Liu for their help in the experiments.

http://dx.doi.org/10.5772/64136

Abbreviations

Abbreviations	Full name
A	Frequency factor
A_{ad}	Ash in air-dried basis
C_{ad}	Carbon in air-dried basis
DSC	Differential scanning colorimetry
DTG	Derivative thermogravimetry
E	Activation energy
FC_{ad}	Fixed carbon in air-dried basis
FTIR	Fourier transform infrared spectroscopy
H_{ad}	Hydrogen in air-dried basis
M	Sample mass
m_0	Initial mass
m_∞	Final mass
M_{ad}	Moisture in air-dried basis
MS	Mass spectrometry
N	Order of reaction
N_{ad}	Nitrogen in air-dried basis
O_{ad}	Oxygen in air-dried basis
PAH	Polycyclic aromatic hydrocarbons
PDF	Power diffraction file
$Q_{ad.net}$	Low calorific capacity in air-dried basis
TG	Thermogravimetric
T_m	Peak flow temperature
T_{ig}	Ignition temperature
T_{max}	Maximum reaction temperature
T_{burn}	Burnout temperature
S_{ad}	Sulfur in air-dried basis
SBC	Shenmu bituminous pulverized coal
V_{ad}	Volatile in air-dried basis
XRD	X-ray diffraction
A	Weight loss ratio
B	Heating rate
R	Gas constant

Author details

Guan-Fu Pan[1,2], Hong-De Xia[1] and Zhen-Yu Tian[1*]

*Address all correspondence to: tianzhenyu@iet.cn

1 Institute of Engineering Thermophysics, Chinese Academy of Sciences, Beijing, China

2 University of Chinese Academy of Sciences, Beijing, China

References

[1] Peng, B.X., Wu, D.S. Study on bromine release from bituminous coal during combustion. Fuel. 2015;157:82–86. DOI: 10.1016/j.fuel.2015.04.059

[2] Tsuji, H., Shirai, H. Matsuda, H. Rajoo, P. Emission characteristics of NOx and unburned carbon in fly ash on high-ash coal combustion. Fuel. 2011;90(2):850–853. DOI: 10.1016/j.fuel.2010.09.053

[3] Molina, A., Shaddix, C.R. Ignition and devolatilization of pulverized bituminous coal particles during oxygen/carbon dioxide coal combustion. Proceedings of the Combustion Institute. 2007;31:1905–1912. DOI: 10.1016/j.proci.2006.08.102

[4] Gao, S.K., Zhang, Y. Meng, J.W., Shu, J.A. Real-time analysis of soot emissions from bituminous coal pyrolysis and combustion with a vacuum ultraviolet photoionization aerosol time-of-flight mass spectrometer. Science of the Total Environment. 2009;407(3):1193–1199. DOI: 10.1016/j.scitotenv.2008.10.026

[5] Yu, Y., Xu, M.H., Yao, H., Yu, D.X., Qiao, Y., Sui, J.C., Liu, X.W., Cao, Q. Char characteristics and particulate matter formation during Chinese bituminous coal combustion. Proceedings of the Combustion Institute. 2007;31:1947–1954. DOI: 10.1016/j.proci.2006.07.116

[6] Cheng, J., Zhou, J.H., Liu, J.Z., Cao, X.Y., Cen, K.F. Transformations and affinities for sulfur of Chinese Shenmu coal ash in a pulverized coal-fired boiler. Energy Sources Part A—Recovery Utilization and Environmental Effects. 2009;31(11):956–966. DOI: 10.1080/15567030802572206

[7] Chang, L.P., Xie, K.C., Li, C.Z. Release of fuel-nitrogen during the gasification of Shenmu coal in O_2. Fuel Processing Technology. 2004;85(8):1053–1063. DOI: 10.1016/j.fuproc.2003.11.038

[8] Wang X.M., Jiao Y.Q., Wu L.Q., Rong H., Wang X.M., Song J. Rare earth element geochemistry and fractionation in Jurassic coal from Dongsheng-Shenmu area, Ordos Basin. Fuel. 2014;136:233–239.

[9] Sun, Q.l., Li, W., Chen, H.K., Li, B.Q. TG-MS study on pyrolysis behavior of Shenmu coal macerals. Journal of China University of Mining & Technology. 2003;32(6):664–669.

[10] Zhao, S.Y. Thermal gravity analysis on combined combustion features of Shenmu coal and semi coke. Coal Science and Technology. 2007;35(7):80–82.

[11] Yang, J.G., Deng, F.R., Zhao, H., Cen, K.F. Mineral conversion and microstructure change in the melting process of Shenmu coal ash. Asia-Pacific Journal of Chemical Engineering. 2007;2(3):165–170. DOI: 10.1002/Apj.036

[12] Yang, W.J., Zhou, J.H., Liu, M.S., ZHou, Z.J., Liu, J.Z., Cen, K.F. Combustion process and nitrogen oxides emission of Shenmu coal added with sodium acetate. Energy & Fuels. 2007;21:2548–2554.

[13] Dijkmans T., Djokic M.R., Van Geem K.M., Marin G.B. Comprehensive compositional analysis of sulfur and nitrogen containing compounds in shale oil using GC × GC-FID/SCD/NCD/TOF-MS. Fuel. 2015;140:398–406.

[14] Yu, Q.M., Pang, Y.J., Chen, H.G. Determination of ignition points in coal-combustion tests. North China Electric Power. 2001;(7):9–10, 50.

[15] Redfern, J.P., Coats, A.W. Kinetic parameters from thermogravimetric data. Nature Biotechnology. 1964;201(4914):68–69.

[16] Xia, H.D., Wei, K. Equivalent characteristic spectrum analysis in TG-MS system. Thermochimica Acta. 2015;602:15–21. DOI: 10.1016/j.tca.2014.12.019

[17] Wang, S.Q., Tang, Y.G., Schobert, H.H., Mitchell, G.D., Liao, F.R., Liu, Z.Z. A thermal behavior study of Chinese coals with high hydrogen content. International Journal of Coal Geology. 2010;81(1):37–44. DOI: 10.1016/j.coal.2009.10.012

[18] Zhang, C.Q., Yu, L.J., Cui, Z.G., Jiang, X.M. Experimental research and computation analysis of combustion kinetic characteristics of micro-pulverized and common-pulverized coal. Journal of Chemical Industry and Engineering. 2005;56(11):2189–2194.

[19] Zhou, Z., Liu, L., Wang, Y.L., Liu, H. Study on the influence of pulverized coal's particle size upon the combustion properties. Thermal Power Generation. 2007;3:35–38, 47.

[20] Lu, H.B., Xu, H.J., Jia, C.X., Zhang, D.L. Experimental study on combustion characteristics of coal in thermogravimetric analyzer. Power System Engineering. 2006;22:11–12, 15.

[21] Nyathi, M.S., Mastalerz, M., Kruse, R. Influence of coke particle size on pore structural determination by optical microscopy. International Journal of Coal Geology. 2013;118:8–14. DOI: 10.1016/j.coal.2013.08.004

[22] Fan, D.M., Zhu, Z.P., Na, Y.J., Lu, Q.G. Thermogravimetric analysis of gasification reactivity of coal chars with steam and CO_2 at moderate temperatures. Journal of Thermal Analysis and Calorimetry. 2012;113:599–607.

[23] Jiang, X.M., Li, J.B., Qiu, J.R. The influence of particle size on compositions analyzing and combustion characteristics of pulverized coal. Journal of China Coal Society. 1999;24:643–647.

[24] Lu, S., Lu, G.J., Jiang, X.G., Chi, Y., Yan, J.H., Cen, K.F., Yu, X.H., Liao, H.Y., Zhao, H. Pyrolysis/combustion characteristics and kinetic analysis of Indonesia lignite sludge. Journal of Coal Science & Engineering. 2014;3:554–561.

[25] Wei, L.H., Jiang, X.M., Yang, T.H., Li, Y.J., Wang, L. Influence of mineral matter on nitrogen conversion in coal during combustion. Acta Scientiae Circumstantiae. 2006;11:1780–1784.

[26] Jiang, X.M., Liu, H., Li, J.B., Zheng, C.G., Liu, D.C. Experimental investigation on sulfur emission properties of micro-pulverized coal. Environmental Science & Technology. 2002;23:126–128.

[27] Ahamad, T., Alshehri, S.M. TG-FTIR-MS (evolved gas analysis) of bidi tobacco powder during combustion and pyrolysis. Journal of Hazardous Materials. 2012;199:200–208. DOI: 10.1016/j.jhazmat.2011.10.090

[28] Silvera, S. TG-FTIR and kinetics of devolatilization of sulcis coal. Journal of Analytical and Applied Pyrolysis. 2013;104:95–102.